

SUPPORTING INFORMATION

Cluster- π electronic interaction in a superatomic Au₁₃ cluster bearing σ -bonded acetylide ligands

Mizuho Sugiuchi,[†] Yukatsu Shichibu,^{†,‡} Takayuki Nakanishi,[§] Yasuchika Hasegawa[§] and Katsuaki Konishi^{†,‡,*}

[†]Graduate School of Environmental Science and [‡]Faculty of Environmental Earth Science, Hokkaido University, North 10 West 5, Sapporo 060-0810 Japan. [§]Faculty of Engineering, Hokkaido University, North 13 West 8, Sapporo 060-8628 Japan.

I. Experimental

A. Materials

Sodium methoxide (95%), ethynylbenzene (97%) were obtained from Wako Pure Chemical Industries. Acetonitrile (99%), methanol (99.5%), ether (99%) and pentane (99%) were purchased from Kanto Chemicals. All the reagents were used as received. [Au₁₃(dppe)₅Cl₂](PF₆)₃ (**1**·(PF₆)₃) was prepared by following the literature procedure.^[1]

B. Measurements

Optical absorption spectra were recorded using a JASCO V-670 double-beam spectrometer. Photoluminescence and excitation spectra were recorded and corrected on a Horiba Scientific SPEX Fluorolog-3ps spectrofluorometer equipped with a Hamamatsu Photonics R928S and R5509 photomultiplier tube detectors. Luminescence lifetimes at 760 nm were measured using Horiba Scientific FluoroCube with a 375 nm pulsed laser diode (NanoLED-375LH) as excitation light source. Electrospray ionization mass (ESI) spectrum was recorded on a Bruker micrOTOF-HS. Crystal data were collected on a Bruker SMART Apex II CCD diffractometer with graphite-monochromated Mo K α radiation ($\lambda = 0.71073 \text{ \AA}$). The crystal structure was solved by direct methods (SHELXS-2013)^[2] and refined by full-matrix least-squares methods on F^2 (SHELXL-2013)^[2] with APEX II software. Non-hydrogen atoms were refined anisotropically. Hydrogen atoms were located at calculated positions and refined isotropically. ³¹P NMR spectrum was collected in CD₃CN at ambient temperature on a JEOL EX-400 NMR spectrometer, and the chemical shifts (in ppm) was referenced to 85% H₃PO₄ (external standard).

C. Syntheses

[Au₁₃(dppe)₅(C≡CPh)₂](PF₆)₃ (**2**·(PF₆)₃): To a mixture of acetonitrile and methanol (2:1 v/v, 40mL) containing [Au₁₃(dppe)₅Cl₂](PF₆)₃ (**1**·(PF₆)₃) (50 mg) were added phenylacetylene (55 μ L; 50 molar eq) and sodium methoxide (26.5 mg; 50 eq) and the resulting solution was stirred for 2 days at room temperature. After the solvents were removed by evaporation, the residue was successively washed with water, diethyl ether, pentane and methanol. The resulting solids were dissolved in acetonitrile and the solution was treated with ether gave analytically pure **2**·(PF₆)₃ as red powders (17.2 mg; 32% based on Au). Red block-shaped crystals of **2**·(PF₆)₃ suitable for X-ray analysis were grown by vapor diffusion of ether into an acetonitrile solution of the cluster. Elemental analysis: calcd (%) for **2**·(PF₆)₃ (C₁₄₆H₁₃₀Au₁₃F₁₈P₁₃): C 33.79, H 2.52; found: C 33.77, H 2.54; no nitrogen was found. ¹H-NMR: δ 1.83-1.90 (m, 10H), 3.50-3.63 (m, 10H), 6.51 (br, 20H), 6.85 (t, 20H), 7.21 (t, 10H), 7.34 (t, 10H), 7.38-7.42 (m, 6H), 7.51 (t, 20H), 7.72-7.77 (br, 4H), 8.47 (br, 20H), ³¹P-NMR: δ 66.88.

II. Computational Details

The calculations of $[\text{Au}_{13}(\text{dppe})_5\text{X}_2]^{3+}$ (**1**: X = Cl; **2**: X = C≡CPh) were performed at density functional theory (DFT) level with TURBOMOLE package.^[3] Geometry optimization and vibrational frequency analysis had been computed at BP86^[4,5] / double- ζ plus polarization (def-SVP)^[6] level. The resolution of the identity (RI) approximation of the coulomb interaction^[7] was used for speeding up. Single-point ground-state calculation was performed at the B3LYP level^[8,9] with basis sets of triple- ζ valence plus polarization quality (def2-TZVP; for Au) and split valence plus polarization quality (def2-SVP; for the other elements).^[10] The same exchange-correlation functional and basis sets were adopted for the subsequent calculations of electronic excitation spectrum using the time-dependent (TD) DFT method. In all calculations, default 60-electron relativistic effective core potential (ECP)^[11] was employed for the Au atom. Crystallographically determined geometric structures of the clusters were used as is for the initial structures of geometry optimization calculations. The fully optimized structures, which were checked to be local minima by frequency calculations, both adopted the C1 symmetry point group.

III. Results

A. Crystal Data of **2·(PF₆)₃·4MeCN·2Et₂O**

Table S1. Crystal data and structure refinement for **2·(PF₆)₃·4MeCN·2Et₂O**.

Empirical formula	C ₁₆₂ H ₁₆₂ Au ₁₃ F ₁₈ N ₄ O ₂ P ₁₃		
Formula weight	5502.12		
Temperature	90 K		
Wavelength	0.71073 Å		
Crystal system	Monoclinic		
Space group	C2/c		
Unit cell dimensions	<i>a</i> = 25.720(2) Å	α = 90°	
	<i>b</i> = 21.2708(18) Å	β = 96.8650(9)°	
	<i>c</i> = 31.007(3) Å	γ = 90°	
Volume	16842(2) Å ³		
<i>Z</i>	4		
Density (calculated)	2.170 Mg/m ³		
Absorption coefficient	11.468 mm ⁻¹		
<i>F</i> (000)	10248		
Crystal size	0.19 x 0.17 x 0.12 mm ³		
Theta range for data collection	1.25 to 26.37°		
Index ranges	-21 ≤ <i>h</i> ≤ 32, -21 ≤ <i>k</i> ≤ 26, -38 ≤ <i>l</i> ≤ 38		
Reflections collected	44566		
Independent reflections	17155 [<i>R</i> (int) = 0.0662]		
Reflections with <i>I</i> > 2σ(<i>I</i>)	8946		
Completeness to theta = 26.37°	99.6 %		
Absorption correction	Empirical		
Max. and min. transmission	0.34 and 0.19		
Refinement method	Full-matrix least-squares on <i>F</i> ²		
Data / restraints / parameters	17155 / 1407 / 945		
Goodness-of-fit on <i>F</i> ²	0.945		
Final <i>R</i> indices [<i>I</i> > 2σ(<i>I</i>)]	<i>R</i> _{<i>I</i>} = 0.0651, <i>wR</i> _{<i>2</i>} = 0.1924		
<i>R</i> indices (all data)	<i>R</i> _{<i>I</i>} = 0.1457, <i>wR</i> _{<i>2</i>} = 0.2604		
Largest diff. peak and hole	4.394 and -5.426 eÅ ⁻³		

B. ORTEP Drawing of $\mathbf{2}\cdot(\text{PF}_6)_3\cdot4\text{MeCN}\cdot2\text{Et}_2\text{O}$

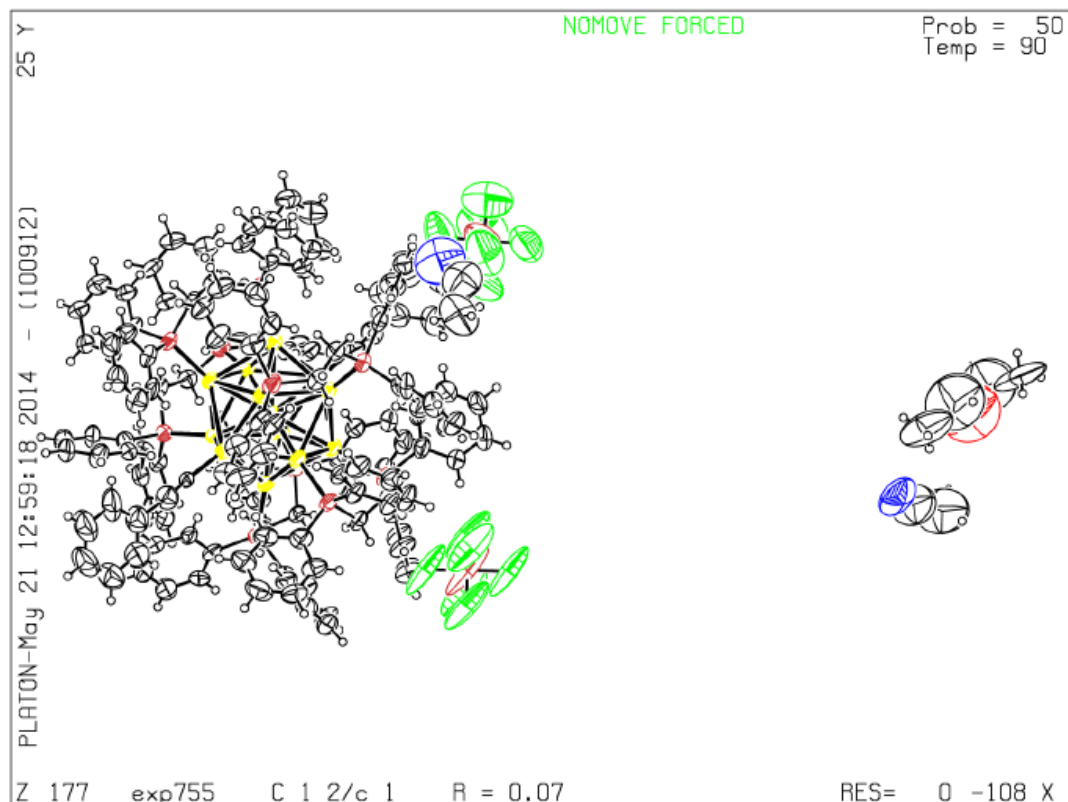


Figure S1. ORTEP drawing of $\mathbf{2}\cdot(\text{PF}_6)_3\cdot4\text{MeCN}\cdot2\text{Et}_2\text{O}$. Thermal ellipsoids are drawn at the 50% probability level.

C. Au - Au Distances

Table S2. Summary of averaged Au-Au bond distances (\AA) of Au_{13} clusters (**1** and **2**).

	$\mathbf{1}\cdot(\text{PF}_6)_3^c$	$\mathbf{2}\cdot(\text{PF}_6)_3$
all Au – Au	2.865	2.861
Au (center) – Au (per. 1) ^{a,b}	2.697 [2.696-2.697]	2.757 [2.757]
Au (center) – Au (per. 2) ^{a,b}	2.777 [2.757-2.798]	2.757 [2.750-2.770]
Au (peripheral) – Au (peripheral) ^{a,b}	2.906 [2.848-2.958]	2.899 [2.861-2.952]

^a Au (per. 1) denotes the peripheral gold atom with chlorido's or alkynyl unit's ligation, and Au (per. 2) does the one with phosphine ligation. ^b The minimum and maximum distances are given in square brackets. ^c ref. 1.

D. ESI mass spectrum

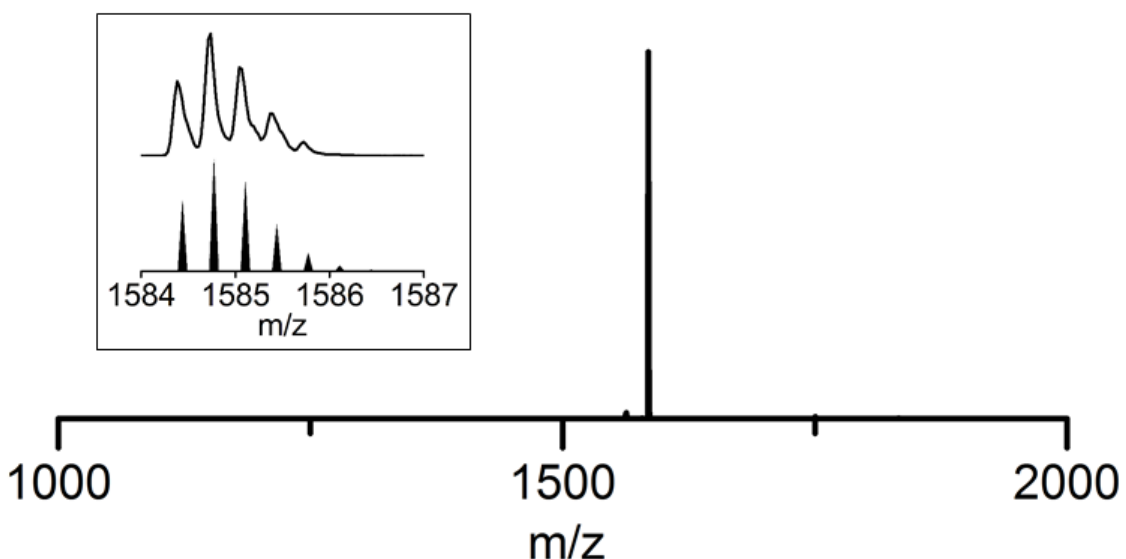


Figure S2. Positive-ion ESI mass spectrum of $\mathbf{2}\cdot(\text{PF}_6)_3$. The inset shows a comparison between the experimental data and the calculated isotope pattern.

E. Optical Absorption Spectra

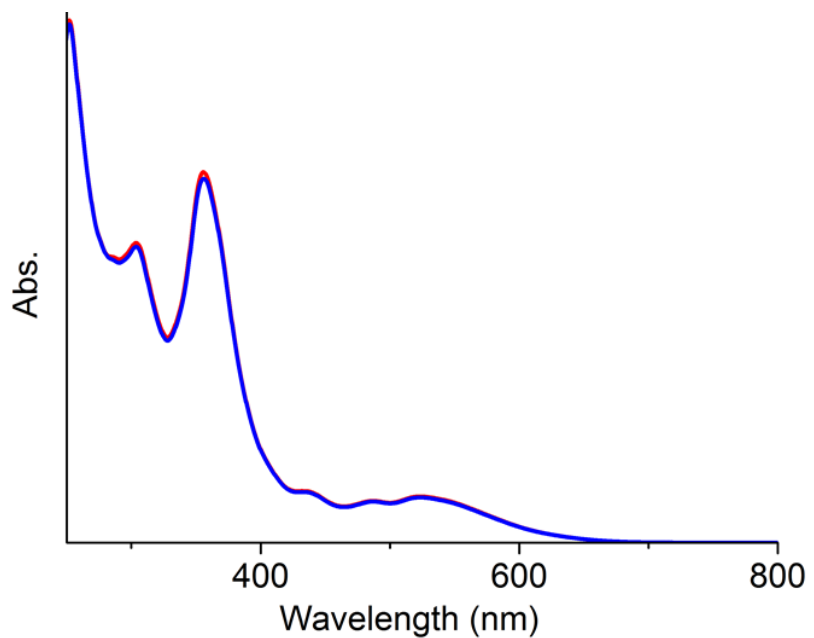


Figure S3. Absorption spectrum of $\mathbf{2}\cdot(\text{PF}_6)_3$ in MeCN for 0 h (red) and 3 weeks (blue).

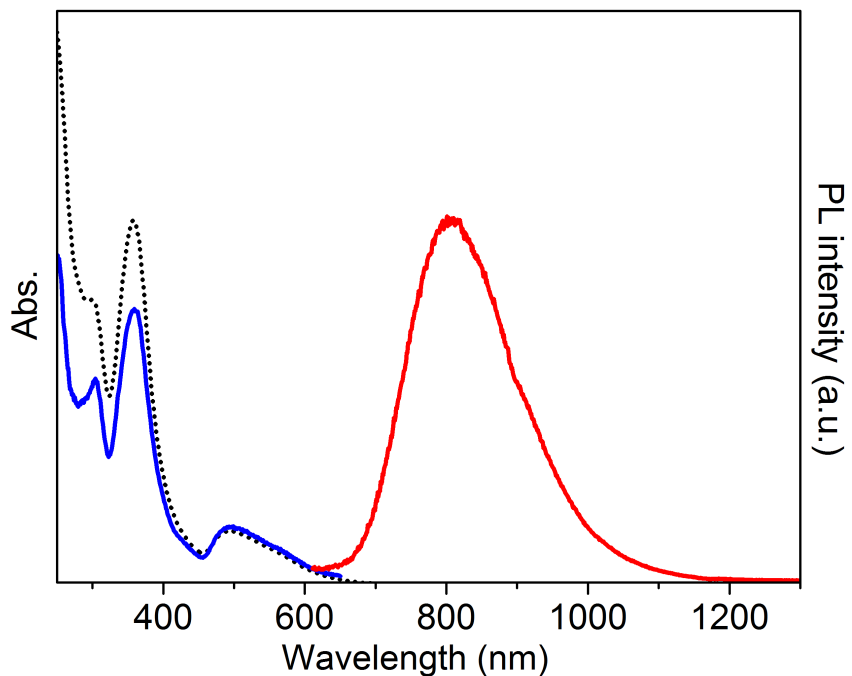


Figure S4. Photoluminescence ($\lambda_{\text{ex}} = 495$ nm; red line) and excitation ($\lambda_{\text{em}} = 800$ nm; blue line) spectra of $\mathbf{1}\cdot(\text{PF}_6)_3$ in MeCN. Its absorption spectrum is also shown as black dotted line.

F. DFT Results

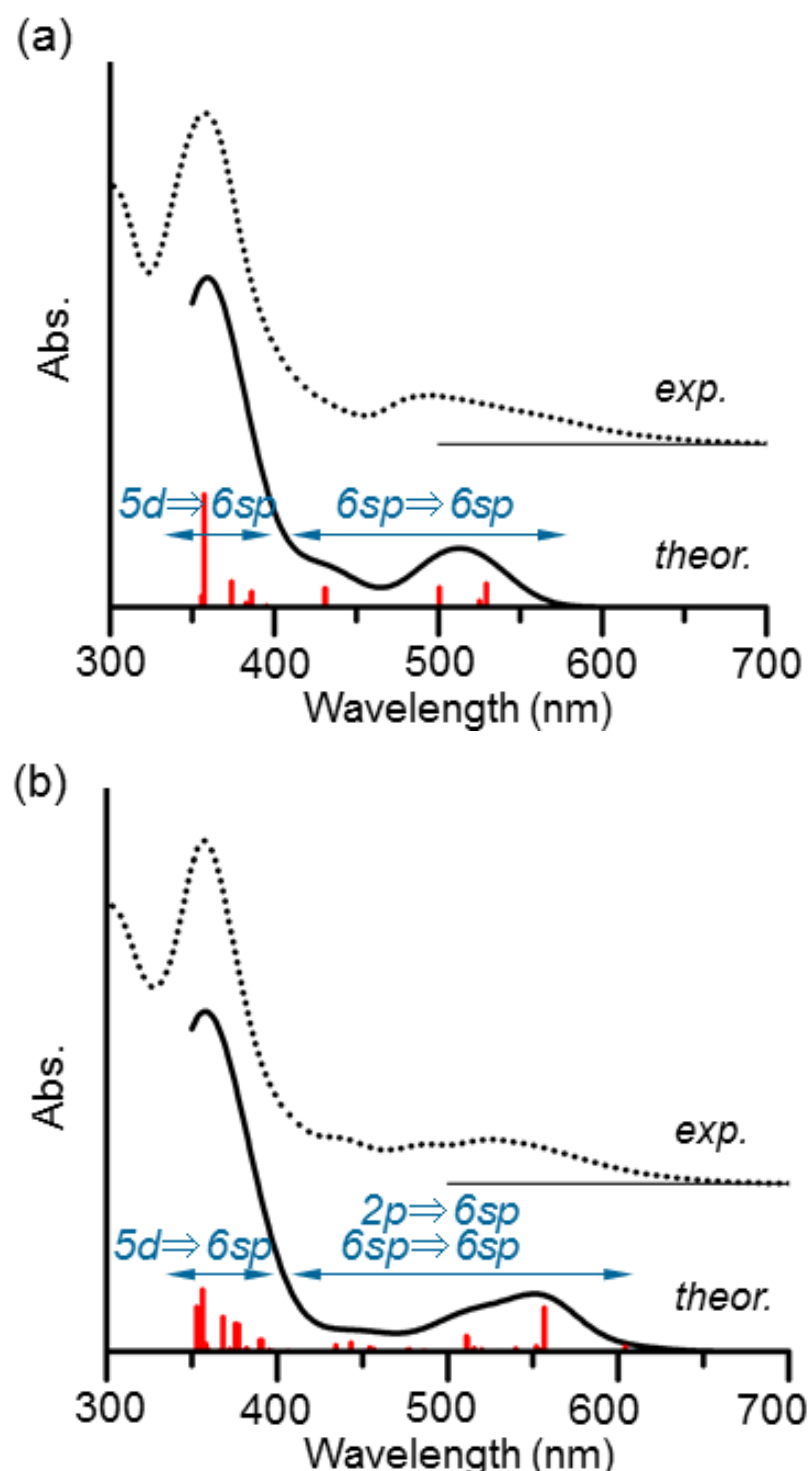


Figure S5. Theoretical absorption spectra (solid lines) of (a) $[\text{Au}_{13}(\text{dppe})_5\text{Cl}_2]^{3+}$ (**1**) and (b) $[\text{Au}_{13}(\text{dppe})_5(\text{C}\equiv\text{CPh})_2]^{3+}$ (**2**). Experimental absorption spectra of them (dotted lines) are shown for comparison.

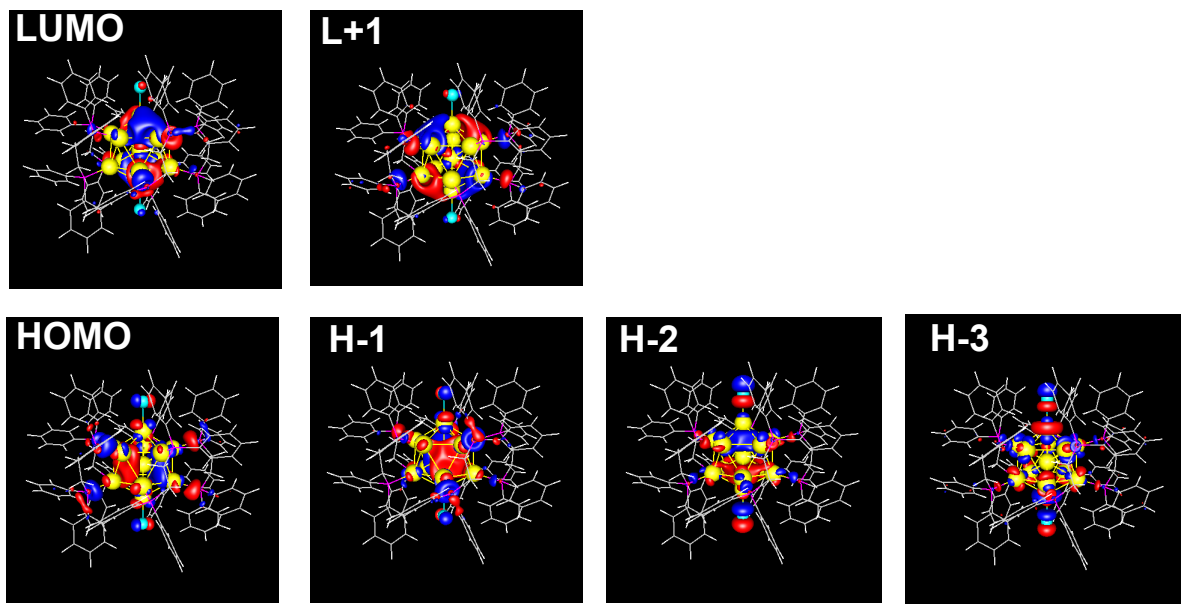


Figure S6. Selected molecular orbitals of **1**.

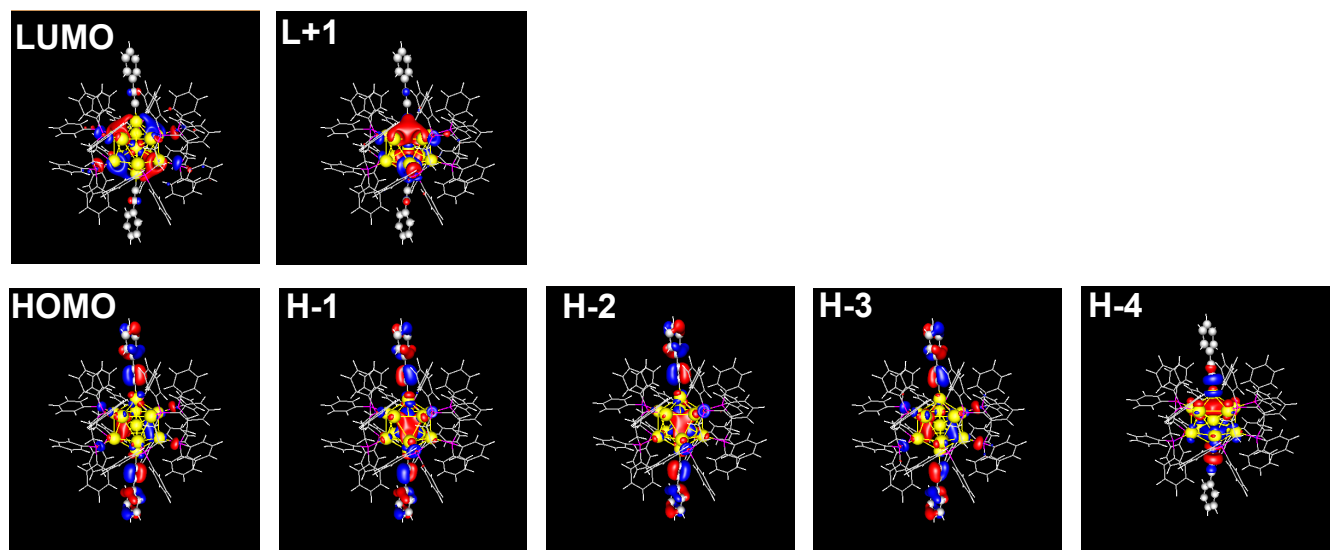


Figure S7. Selected molecular orbitals of **2**.

Table S3. Kohn-Sham orbitals, energies, and atomic orbital contributions of $[\text{Au}_{13}(\text{dppe})_5\text{Cl}_2]^{3+}$ (**1**).

MO	Orbital index	Orbital energy (eV) / Relative energy (eV)	% Au (sp)	% Au (d)	% P (p)	% Cl (p)
LUMO+8	673a	-6.12 / 3.98	47	0	12	0
LUMO+7	672a	-6.13 / 3.98	48	0	13	0
LUMO+6	671a	-6.37 / 3.73	64	1	13	0
LUMO+5	670a	-6.37 / 3.73	64	1	13	0
LUMO+4	669a	-7.00 / 3.11	61	19	6	11
LUMO+3	668a	-7.16 / 2.95	70	3	13	0
LUMO+2	667a	-7.16 / 2.95	70	3	13	0
LUMO+1	666a	-7.29 / 2.82	70	0	13	1
LUMO	665a	-7.29 / 2.82	70	0	13	1
HOMO	664a	-10.11 / 0.00	47	11	19	4
HOMO-1	663a	-10.11 / 0.00	46	14	19	4
HOMO-2	662a	-10.77 / -0.67	42	16	8	22
HOMO-3	661a	-11.10 / -0.99	11	40	12	13
HOMO-4	660a	-11.16 / -1.06	11	33	18	0
HOMO-5	659a	-11.16 / -1.06	11	32	18	0
HOMO-6	658a	-11.30 / -1.19	9	26	5	39
HOMO-7	657a	-11.30 / -1.19	9	26	5	40
HOMO-8	656a	-11.48 / -1.38	10	14	0	54
HOMO-9	655a	-11.48 / -1.38	9	14	0	54
HOMO-10	654a	-11.57 / -1.46	13	22	0	6
HOMO-11	653a	-11.57 / -1.46	10	8	1	23
HOMO-12	652a	-11.57 / -1.47	10	9	2	23
HOMO-13	651a	-11.60 / -1.49	8	7	2	0
HOMO-14	650a	-11.60 / -1.49	8	7	2	0

Table S4. Excited states, energies, oscillator strengths, and primary orbital-orbital transitions of $[\text{Au}_{13}(\text{dppe})_5\text{Cl}_2]^{3+}$ (**1**).

Excitation index	Energy (eV) / Wavelength (nm)	Oscillator strength	Dominant transition	Nature of transition
1	2.31 / 536	0.0001	664a→667a, 663a→668a	HOMO→LUMO+2, HOMO-1→LUMO+3
2	2.34 / 529	0.1010	664a→666a, 663a→665a	HOMO→LUMO+1, HOMO-1→LUMO
3	2.36 / 525	0.0252	664a→669a, 663a→668a, 664a→667a	HOMO→LUMO+4, HOMO-1→LUMO+3, HOMO→LUMO+2
4	2.36 / 525	0.0254	663a→669a, 664a→668a, 663a→667a	HOMO-1→LUMO+4, HOMO→LUMO+3, HOMO-1→LUMO+2
5	2.48 / 501	0.0834	663a→669a	HOMO-1→LUMO+4
6	2.48 / 501	0.0838	664a→669a	HOMO→LUMO+4
7	2.88 / 431	0.0816	662a→665a	HOMO-2→LUMO
8	2.88 / 431	0.0811	662a→666a	HOMO-2→LUMO+1
9	3.14 / 395	0.0043	664a→670a	HOMO→LUMO+5
10	3.14 / 395	0.0052	663a→670a, 664a→671a	HOMO-1→LUMO+5, HOMO→LUMO+6
11	3.14 / 395	0.0001	664a→671a, 663a→670a	HOMO→LUMO+6, HOMO-1→LUMO+5
12	3.14 / 395	0.0005	663a→671a	HOMO-1→LUMO+6
13	3.21 / 386	0.0657	661a→665a	HOMO-3→LUMO
14	3.21 / 386	0.0628	661a→666a	HOMO-3→LUMO+1
15	3.24 / 383	0.0161	662a→669a	HOMO-2→LUMO+4
16	3.28 / 378	0.0002	660a→665a, 659a→666a	HOMO-4→LUMO, HOMO-5→LUMO+1
17	3.28 / 378	0.0001	659a→665a, 660a→666a	HOMO-5→LUMO, HOMO-4→LUMO+1
18	3.32 / 374	0.1082	660a→666a, 659a→665a	HOMO-4→LUMO+1, HOMO-5→LUMO
19	3.32 / 374	0.1100	659a→666a, 660a→665a	HOMO-5→LUMO+1, HOMO-4→LUMO
20	3.35 / 370	0.0003	659a→668a, 660a→667a	HOMO-5→LUMO+3, HOMO-4→LUMO+2
21	3.38 / 366	0.0007	658a→665a, 664a→672a	HOMO-6→LUMO, HOMO→LUMO+7
22	3.44 / 360	0.0002	663a→673a, 657a→666a	HOMO-1→LUMO+8, HOMO-7→LUMO+1
23	3.47 / 357	0.4902	659a→667a, 660a→668a	HOMO-5→LUMO+2, HOMO-4→LUMO+3
24	3.47 / 357	0.4916	659a→668a, 660a→667a	HOMO-5→LUMO+3, HOMO-4→LUMO+2
25	3.49 / 356	0.0463	660a→668a, 659a→667a	HOMO-4→LUMO+3, HOMO-5→LUMO+2

Table S5. Kohn-Sham orbitals, energies, and atomic orbital contributions of $[\text{Au}_{13}(\text{dppe})_5(\text{C}\equiv\text{CPh})_2]^{3+}$ (**2**).

MO	Orbital index	Orbital energy (eV) / Relative energy (eV)	% Au (sp)	% Au (d)	% P (p)	% C_CC (p) ^a	% C_Ph (p) ^a
LUMO+15	716a	-5.76 / 4.00	5	0	7	0	0
LUMO+14	715a	-5.77 / 4.00	3	0	6	0	0
LUMO+13	714a	-5.77 / 3.99	4	0	5	0	0
LUMO+12	713a	-5.79 / 3.98	4	0	7	0	0
LUMO+11	712a	-5.80 / 3.96	0	0	8	0	0
LUMO+10	711a	-5.81 / 3.95	1	0	6	0	0
LUMO+9	710a	-5.81 / 3.95	0	0	7	0	0
LUMO+8	709a	-6.01 / 3.75	48	0	12	2	0
LUMO+7	708a	-6.02 / 3.75	50	0	12	2	0
LUMO+6	707a	-6.18 / 3.58	61	1	13	0	0
LUMO+5	706a	-6.18 / 3.58	61	1	13	0	0
LUMO+4	705a	-6.40 / 3.36	64	8	10	5	0
LUMO+3	704a	-6.99 / 2.77	70	3	13	0	0
LUMO+2	703a	-7.00 / 2.77	70	3	13	0	0
LUMO+1	702a	-7.17 / 2.59	70	0	12	2	0
LUMO	701a	-7.18 / 2.58	68	0	12	2	0
HOMO	700a	-9.76 / 0.00	24	10	7	25	25
HOMO-1	699a	-9.85 / -0.09	27	8	9	23	22
HOMO-2	698a	-10.05 / -0.29	22	7	9	24	27
HOMO-3	697a	-10.20 / -0.44	27	5	12	18	25
HOMO-4	696a	-10.21 / -0.45	44	24	2	14	0
HOMO-5	695a	-10.79 / -1.03	5	16	1	68	2
HOMO-6	694a	-10.88 / -1.12	0	0	0	0	97
HOMO-7	693a	-10.88 / -1.12	0	0	0	0	98
HOMO-8	692a	-10.89 / -1.13	8	10	2	66	3
HOMO-9	691a	-10.91 / -1.15	14	35	17	4	0
HOMO-10	690a	-11.01 / -1.25	11	37	18	0	0
HOMO-11	689a	-11.02 / -1.25	11	36	19	0	0

^a % C_CC (p) and % C_Ph (p) denote the relative contributions of C (2p) atomic orbitals for C≡C and Ph in C≡CPh units, respectively.

Table S6. Excited states, energies, oscillator strengths, and primary orbital-orbital transitions of $[\text{Au}_{13}(\text{dppe})_5(\text{C}\equiv\text{CPh})_2]^{3+}$ (**2**).

Excitation index	Energy (eV) / Wavelength (nm)	Oscillator strength	Dominant transition	Nature of transition
1	2.05 / 604	0.0238	700a→701a, 699a→702a	HOMO→LUMO, HOMO-1→LUMO+1
2	2.23 / 557	0.2261	699a→702a, 700a→701a	HOMO-1→LUMO+1, HOMO→LUMO
3	2.24 / 555	0.0078	700a→703a	HOMO→LUMO+2
4	2.25 / 552	0.0254	700a→704a	HOMO→LUMO+3
5	2.30 / 540	0.0043	699a→704a, 696a→701a	HOMO-1→LUMO+3, HOMO-4→LUMO
6	2.30 / 540	0.0134	699a→703a, 696a→702a	HOMO-1→LUMO+2, HOMO-4→LUMO+1
7	2.39 / 520	0.0100	698a→702a	HOMO-2→LUMO+1
8	2.41 / 516	0.0172	698a→701a	HOMO-2→LUMO
9	2.42 / 512	0.0684	696a→701a, 699a→704a	HOMO-4→LUMO, HOMO-1→LUMO+3
10	2.43 / 511	0.0772	696a→702a, 699a→703a	HOMO-4→LUMO+1, HOMO-1→LUMO+2
11	2.53 / 490	0.0004	696a→703a	HOMO-4→LUMO+2
12	2.54 / 487	0.0019	696a→704a	HOMO-4→LUMO+3
13	2.55 / 486	0.0031	697a→701a	HOMO-3→LUMO
14	2.60 / 478	0.0102	698a→703a	HOMO-2→LUMO+2
15	2.60 / 476	0.0080	698a→704a	HOMO-2→LUMO+3
16	2.72 / 457	0.0118	697a→703a	HOMO-3→LUMO+2
17	2.73 / 454	0.0184	697a→704a	HOMO-3→LUMO+3
18	2.80 / 443	0.0445	700a→705a	HOMO→LUMO+4
19	2.85 / 434	0.0293	699a→705a	HOMO-1→LUMO+4
20	3.05 / 407	0.0020	695a→701a	HOMO-5→LUMO
21	3.08 / 403	0.0007	700a→706a	HOMO→LUMO+5
22	3.08 / 403	0.0010	700a→707a	HOMO→LUMO+6
23	3.12 / 397	0.0020	698a→705a	HOMO-2→LUMO+4
24	3.14 / 395	0.0071	699a→707a, 691a→701a	HOMO-1→LUMO+6, HOMO-9→LUMO
25	3.14 / 395	0.0009	699a→706a	HOMO-1→LUMO+5
26	3.17 / 391	0.0564	691a→701a, 699a→707a	HOMO-9→LUMO, HOMO-1→LUMO+6
27	3.18 / 390	0.0044	692a→701a	HOMO-8→LUMO
28	3.18 / 390	0.0580	691a→702a	HOMO-9→LUMO+1
29	3.20 / 387	0.0010	692a→702a	HOMO-8→LUMO+1
30	3.24 / 383	0.0040	690a→701a, 689a→702a	HOMO-10→LUMO, HOMO-11→LUMO+1
31	3.24 / 383	0.0008	689a→701a, 690a→702a	HOMO-11→LUMO, HOMO-10→LUMO+1
32	3.25 / 382	0.0154	697a→705a, 690a→702a	HOMO-3→LUMO+4, HOMO-10→LUMO+1
33	3.26 / 380	0.0030	700a→709a	HOMO→LUMO+8
34	3.27 / 379	0.0023	700a→708a	HOMO→LUMO+7
35	3.28 / 378	0.0004	695a→703a	HOMO-5→LUMO+2
36	3.28 / 378	0.1382	689a→702a, 690a→701a	HOMO-11→LUMO+1, HOMO-10→LUMO
37	3.29 / 376	0.0188	695a→704a	HOMO-5→LUMO+3
38	3.30 / 376	0.1424	690a→702a, 697a→705a	HOMO-10→LUMO+1, HOMO-3→LUMO+4
39	3.32 / 374	0.0033	691a→703a	HOMO-9→LUMO+2
40	3.33 / 373	0.0013	691a→704a	HOMO-9→LUMO+3
41	3.33 / 372	0.0107	699a→708a	HOMO-1→LUMO+7
42	3.36 / 369	0.0022	690a→703a, 689a→704a	HOMO-10→LUMO+2, HOMO-11→LUMO+3
43	3.37 / 368	0.1766	696a→705a	HOMO-4→LUMO+4

44	3.38 / 366	0.0002	693a→701a, 694a→701a	HOMO-7→LUMO, HOMO-6→LUMO
45	3.38 / 366	0.0002	694a→701a, 693a→701a	HOMO-6→LUMO, HOMO-7→LUMO
46	3.39 / 366	0.0017	692a→703a	HOMO-8→LUMO+2
47	3.39 / 365	0.0001	694a→702a, 693a→702a	HOMO-6→LUMO+1, HOMO-7→LUMO+1
48	3.40 / 364	0.0011	692a→704a	HOMO-8→LUMO+3
49	3.42 / 363	0.0002	698a→707a	HOMO-2→LUMO+6
50	3.44 / 360	0.0020	696a→707a	HOMO-4→LUMO+6
51	3.44 / 360	0.0048	696a→706a, 698a→706a	HOMO-4→LUMO+5, HOMO-2→LUMO+5
52	3.46 / 358	0.0260	687a→701a	HOMO-13→LUMO
53	3.46 / 358	0.0401	687a→702a	HOMO-13→LUMO+1
54	3.48 / 356	0.3209	690a→704a, 689a→703a	HOMO-10→LUMO+3, HOMO-11→LUMO+2
55	3.48 / 356	0.3027	689a→704a	HOMO-11→LUMO+3
56	3.51 / 353	0.2303	690a→704a, 689a→703a	HOMO-10→LUMO+3, HOMO-11→LUMO+2

References

- [1] Y. Shichibu, K. Konishi, *Small* **2010**, *6*, 1216.
- [2] G. M. Sheldrick, *Acta Cryst.* **2008**, *A64*, 112.
- [3] TURBOMOLE V6.3 2011, a development of University of Karlsruhe and Forschungszentrum Karlsruhe GmbH, 1989-2007, TURBOMOLE GmbH, since 2007; available from <http://www.turbomole.com>.
- [4] A. D. Becke, *Phys. Rev. A*, **1988**, *38*, 3098.
- [5] J. P. Perdew, *Phys. Rev. B*, **1986**, *33*, 8822.
- [6] A. Schäfer, H. Horn and R. Ahlrichs, *J. Chem. Phys.*, **1992**, *97*, 2571.
- [7] R. Ahlrichs, M. Bar, M. Haser, H. Horn and C. Kolmel, *Chem. Phys. Lett.*, **1989**, *162*, 165.
- [8] C. Lee, W. Yang and R. G. Parr, *Phys. Rev. B*, **1988**, *37*, 785.
- [9] A. D. Becke, *J. Chem. Phys.*, **1993**, *98*, 5648.
- [10] F. Weigend and R. Ahlrichs, *Phys. Chem. Chem. Phys.*, **2005**, *7*, 3297.
- [11] D. Andrae, U. Häuerßmann, M. Dolg, H. Stoll and H. Preuß, *Theor. Chim. Acta*, **1990**, *77*, 123.